Simultaneous generation of second to fifth harmonic conical beams in a two dimensional nonlinear photonic crystal

Luis Mateos,[1] Pablo Molina,[1] Juan Galisteo,[2] Cefe López,[2] Luisa E. Bausá,[1] and Mariola O Ramírez[1,*]

[1]*Dpto. Física de Materiales and Instituto Nicolás Cabrera, Universidad Autónoma de Madrid 28049 Madrid, Spain*
[2]*Instituto de Ciencia de Materiales de Madrid (CSIC), Calle Sor Juana Inés de la Cruz, 28049 Madrid, Spain*
[*]*mariola.ramirez@uam.es*

Abstract: Broadly tunable multiple high-harmonic conical beams have been generated by means of a multistep $\chi^{(2)}$ cascade processes in a two dimensional nonlinear photonic crystal. The nonlinear structure consists of a square lattice of inverted hexagonal domains with diameters and distances between domains as low as 1 μm. The large number of reciprocal lattice vectors provided by both the square nonlinear structure and the hexagonal shaped domains, along with imperfections on the size and shape of the individual domains make possible the simultaneous generation of second up to fifth harmonic conical beams in a single nonlinear structure by using different types of phase matching geometries. The frequency response can be tuned in an extremely large spectral range, and continuous generation of nonlinear conical beams covering the whole visible spectral region can be achieved. Further, the same photon energy can be generated at different orders, so that concentrically emitted conical beams with angular dispersion as large as $\Delta\theta = 50°$ can be observed. The results highlight the significance of highly controlled engineered 2D nonlinear structures to generate advanced multi-photon devices with large spatial and spectral tunable response.

OCIS codes: (190.0190) Nonlinear optics; (190.2620) Harmonic generation and mixing; (190.4160) Multiharmonic generation; (160.4330) Nonlinear optical materials; (130.3730) Lithium niobate; (160.2260) Ferroelectrics.

References and links

1. P. Ferraro, S. Grilli, and P. De Natale, *Ferroelectric Crystals for Photonic Applications* (Springer Series in Materials Science 2009).
2. S. N. Zhu, Y. Y. Zhu, and N. B. Ming, "Quasi-phase-matched third-harmonic generation in a quasi-periodic optical superlattice," Science **278**(5339), 843–846 (1997).
3. C. Canalias and V. Pasiskevicius, "Mirrorles optical parametric oscillator," Nat. Photonics **1**(8), 459–462 (2007).
4. J. L. He, J. Liao, H. Liu, J. Du, F. Xu, H. T. Wang, S. N. Zhu, Y. Y. Zhu, and N. B. Ming, "Simultaneous cw red, yellow, and green light generation, "traffic signal lights", by frequency doubling and sum-frequency mixing in an aperiodically poled $LiTaO_3$," Appl. Phys. Lett. **83**(2), 228–230 (2003).
5. C. Canalias, V. Pasiskevicius, M. Fokine, and F. Laurell, "Backward quasi-phase matched second harmonic generation in sub-micrometer periodically poled flux-grown $KTiOPO_4$," Appl. Phys. Lett. **86**(18), 181105 (2005).
6. L. E. Myers, R. C. Eckardt, M. M. Fejer, R. L. Byer, W. R. Bosenberg, and J. W. Pierce, "Quasi-phase-matched optical parametric oscillators in bulk periodically poled $LiNbO_3$," J. Opt. Soc. Am. B **12**(11), 2102–2106 (1995).
7. V. Berger, "Nonlinear photonic crystals," Phys. Rev. Lett. **81**(19), 4136–4139 (1998).
8. T. Ellenbogen, N. Voloch-Bloch, A. Ganany-Padowicz, and A. Arie, "Nonlinear generation and manipulation of Airy beams," Nat. Photonics **3**(7), 395–398 (2009).
9. N. G. R. Broderick, R. T. Bratfalean, T. M. Monro, D. J. Richardson, and C. M. de Sterke, "Temperature and wavelength tuning of second-, third-, and fourth-harmonic generation in a two-dimensional hexagonally poled nonlinear crystal," J. Opt. Soc. Am. B **19**(9), 2263–2272 (2002).
10. R. Lifshitz, A. Arie, and A. Bahabad, "Photonic quasicrystals for nonlinear optical frequency conversion," Phys. Rev. Lett. **95**(13), 133901 (2005).

#179795 - $15.00 USD Received 12 Nov 2012; revised 8 Dec 2012; accepted 17 Dec 2012; published 21 Dec 2012

11. K. Gallo, M. Levenius, F. Laurell, and V. Pasiskevicius, "Twin-beam optical parametric generation in $\chi^{(2)}$ nonlinear photonic crystals," Appl. Phys. Lett. **98**(16), 161113 (2011).
12. M. B. Nasr, S. Carrasco, B. E. A. Saleh, A. V. Sergienko, M. C. Teich, J. P. Torres, L. Torner, D. S. Hum, and M. M. Fejer, "Ultrabroadband biphotons generated via chirped quasi-phase-matched optical parametric down-conversion," Phys. Rev. Lett. **100**(18), 183601 (2008).
13. C. Langrock, S. Kumar, J. E. McGeehan, A. E. Willner, and M. M. Fejer, "All-optical signal processing using χ^2 nonlinearities in guided –wave devices," J. Lightwave Technol. **24**(7), 2579–2592 (2006).
14. X. C. Yao, T. X. Wang, P. Xu, H. Lu, G. S. Pan, X. H. Bao, C. Z. Peng, C. Y. Lu, Y. A. Chen, and J. W. Pan, "Observation of eight photon entanglement," Nat. Photonics **6**(4), 225–228 (2012).
15. Y. Sheng, A. Best, H. J. Butt, W. Krolikowski, A. Arie, and K. Koynov, "Three-dimensional ferroelectric domain visualization by Cerenkov-type second harmonic generation," Opt. Express **18**(16), 16539–16545 (2010).
16. S. M. Saltiel, D. N. Neshev, R. Fischer, W. Krolikowski, A. Arie, and Y. S. Kivshar, "Generation of second-harmonic conical waves via nonlinear bragg diffraction," Phys. Rev. Lett. **100**(10), 103902 (2008).
17. N. An, H. Ren, Y. Zheng, X. Deng, and X. Chen, "Cherenkov high-order harmonic generation by multistep cascading in chi((2)) nonlinear photonic crystal," Appl. Phys. Lett. **100**(22), 221103 (2012).
18. P. Molina, M. O. Ramirez, and L. E. Bausa, "Strontium barium niobate as a multifunctional two-dimensional nonlinear "photonic glass"," Adv. Funct. Mater. **18**(5), 709–715 (2008).
19. S. M. Saltiel, Y. Sheng, N. Voloch-Bloch, D. N. Neshev, W. Krolikowski, A. Arie, K. Koynov, and Y. S. Kivshar, "Cerenkov-type second-harmonic generation in two-dimensional nonlinear photonic structures," IEEE J. Quantum Electron. **45**(11), 1465–1472 (2009).
20. P. Molina, M. O. Ramirez, B. J. Garcia, and L. E. Bausa, "Directional dependence of the second harmonic response in two-dimensional nonlinear photonic crystals," Appl. Phys. Lett. **96**(26), 261111 (2010).
21. D. E. Zelmon, D. L. Small, and D. Jundt, "Infrared corrected Sellmeier coefficients for congruently grown lithium niobate and 5 mol. % magnesium oxide–doped lithium niobate," J. Opt. Soc. Am. B **14**(12), 3319–3322 (1997).
22. Y. Sheng, W. Wang, R. Shiloh, V. Roppo, Y. Kong, A. Arie, and W. Krolikowski, "Cerenkov third-harmonic generation in chi((2)) nonlinear photonic crystal," Appl. Phys. Lett. **98**(24), 241114 (2011).
23. H. X. Li, S. Y. Mu, P. Xu, M. L. Zhong, C. D. Chen, X. P. Hu, W. N. Cui, and S. N. Zhu, "Multicolor Cerenkov conical beams generation by cascaded- chi((2)) processes in radially poled nonlinear photonic crystals," Appl. Phys. Lett. **100**(10), 101101 (2012).
24. M. Ayoub, P. Roedig, J. Imbrock, and C. Denz, "Cascaded Čerenkov third-harmonic generation in random quadratic media," Appl. Phys. Lett. **99**(24), 241109 (2011).
25. A. Pasquazi, A. Busacca, S. Stivala, R. Morandotti, and G. Assanto, "Nonlinear disorder mapping through three-wave mixing," IEEE Photon. J. **2**(1), 18–28 (2010).
26. Y. Sheng, W. Wang, R. Shiloh, V. Roppo, A. Arie, and W. Krolikowski, "Third-harmonic generation via nonlinear Raman-Nath diffraction in nonlinear photonic crystal," Opt. Lett. **36**(16), 3266–3268 (2011).
27. T. Ellenbogen, A. Ganany-Padowicz, and A. Arie, "Nonlinear photonic structures for all-optical deflection," Opt. Express **16**(5), 3077–3082 (2008).
28. L. Mateos, P. Molina, L. E. Bausa, and M. O. Ramirez, "Second harmonic conical waves for symmetry studies in chi((2)) nonlinear photonic crystals," Appl. Phys. Express **4**(8), 082202 (2011).
29. Y. Sheng, A. Best, H. J. Butt, W. Krolikowski, A. Arie, and K. Koynov, "Three-dimensional ferroelectric domain visualization by Čerenkov-type second harmonic generation," Opt. Express **18**(16), 16539–16545 (2010).
30. A. Rossi, G. Vallone, A. Chiuri, F. De Martini, and P. Mataloni, "Multipath entanglement of two photons," Phys. Rev. Lett. **102**(15), 153902 (2009).

1. Introduction

Frequency conversion processes based on domain engineered ferroelectric crystals have shown to be an effective approach to generate compact sources of radiation capable to operate in a broad spectral range [1]. A large variety of nonlinear optical phenomena including sum-frequency mixing, optical parametric oscillation or even backwards second harmonic generation (SHG) have been successfully demonstrated by using periodically poled structures to quasi-phase-match (QPM) optical interactions [2–6]. Moreover, the QPM generalization from one to two dimensional $\chi^{(2)}$ modulation – the so-called two dimensional nonlinear photonic crystals (2DNLPC), expanded the access to several reciprocal lattice vectors within the same crystal, increasing not only the frequency range suitable to be converted but also the directions at which the nonlinear processes take place [7]. Besides, simultaneous phase matching (PM) of multiple nonlinear interactions can also be supported by the 2D nonlinear structures as demonstrated in several theoretical and experimental works [8–11]. The performance of these devices strongly depends on the shapes and sizes of ferroelectric domains, which is ultimately determined by the ability to engineer domain structures with precision. In fact, alternate ferroelectric domains structures with increasingly smaller sizes

#179795 - $15.00 USD Received 12 Nov 2012; revised 8 Dec 2012; accepted 17 Dec 2012; published 21 Dec 2012

and periods are ever more required to control the generation and light distribution in several scientific and technologically relevant fronts. Telecommunications, sensing applications or quantum optics are some examples of multidisciplinary fields, where not only large spatial and spectral tunability, but also multiphoton operation, are currently demanded [12–14]. Here, we have fabricated a square lattice of ~1 μm size alternate ferroelectric domains with a poling period Λ~2 μm and a fractional filling factor $f = 0.35$ (Fig. 1(a)), to demonstrate what we believe to be the highest tunable multistep cascaded $\chi^{(2)}$ conical harmonic generation up to date in a solid state system. Such a short domain periodicity in $LiNbO_3$ is the result of a technological improvement on ferroelectric domain engineering provided by the use of direct electron beam writing (DEBW) as a tool to reverse the spontaneous polarization. From SHG up to fifth harmonic generation (FiHG) are simultaneously generated in a conical geometry by means of a single fundamental beam. The harmonic waves are generated at different conical angles and an extremely large tunability range ($\Delta\lambda$>1000 nm), only limited by the experimental set-up, is demonstrated without any angle or thermal tunning of the nonlinear structure. Further, we show how the short poling period along with the extensive spatial control of the fabricated nonlinear structure allows the PM condition to be fulfilled at numerous *m,n* diffraction orders. As a result, the generation of multiple high harmonic conical waves exhibiting angular dispersion values as large as $\Delta\theta = 50°$ for a fixed frequency converted wavelength is achieved. Together, all these results highlight the significance of highly controlled engineered 2D nonlinear structures to generate broadly tunable multi-photon devices with marked dispersive properties in extremely large spectral ranges (400-1000 nm).

2. Experimental

The ferroelectric domain pattern was fabricated by means of direct electron beam writing (DEBW). The electron beam was focused on the -z face of the crystal by means of a Philips XL30 Schottky field emission gun electron microscope driven by an Elphy Raith nanolithography software. Prior to the irradiation process, a 0.5 mm thick z-cut congruent $LiNbO_3$ a 100nm Al film was deposited on the + z face, which acted as a ground electrode.The irradiation process was performed without any mask. The acceleration voltage was 15 kV and the applied charge density 1500 μC/cm^2. The inverted domains grew along the polar axis of the crystal (*z* axis) and crossed the whole thickness of the sample. The diameter of the inverted domains in the *xy* plane was 1 μm and the lattice parameter of the two dimensional square lattice was $\Lambda = 2$ μm. The average filling factor, *f,* defined as the ratio of the total inverted area to the original polarization area was $f = 0.35$ in both. The spatial extension of the patterns was 0.5x0.5 mm^2. The inverted ferroelectric domain structures were revealed after a selective chemical etching in a 2:1 solution of HNO_3:HF. For the high harmonic generation experiments, the sample was polished up to optical quality. An ultrafast optical parametric amplifier (OPerA-Solo (COHERENT)) generating 140 fs pulses at a repetition rate of 1 kHz was used as tunable excitation source in the 1200-2400 nm spectral range. The average output power was 100 mW. The laser beam was linearly polarized. All the frequency conversion experiments were performed with the fundamental beam travelling parallel to the ferroelectric axis. The multicolour concentric circular rings generated by the conical beams were projected on a screen. Half wave-plates were used to control the laser polarization. The pictures of the generated conical radiation were obtained by means of Nikon D90 digital camera.

3. Results and discussion

The frequency conversion experiments were performed with the fundamental beam travelling parallel to the ferroelectric axis, and so to the domain walls. Upon this configuration the enhanced second order nonlinearity induced by domain walls [15–20], was exploited to generate $\chi^{(2)}$ parametric processes resulting in broadband generation of multiple high-harmonic conical beams (from second to fifth order). These consisted of multicolour

#179795 - $15.00 USD Received 12 Nov 2012; revised 8 Dec 2012; accepted 17 Dec 2012; published 21 Dec 2012

concentric circular rings, which were projected on a graph paper screen. A schematic of the experimental setup is shown in Fig. 1(b). The experimental images obtained for four different fundamental wavelengths (1450, 1900, 2100 and 2300nm respectively) are shown in Fig. 1(c-f). As seen, as the fundamental wavelength is tuned, the harmonic conical waves are generated at different frequencies and emission angles defined by the PM geometry involved in the $\chi^{(2)}$ cascade process. All the conical generated beams show the azimuthal intensity dependence related to that of the quadratic nonlinear effective coefficients d_{eff} of $LiNbO_3$. This fact, along with the presence of two closely separated rings at the same frequency (ordinary and extraordinary beams) arises from the anisotropy of $LiNbO_3$ and has been treated in previous work [19, 20]. Additionally, due to the high peak power of the incident beam, collinear SHG and THG generation are also obtained even when the PM condition is not rigorously satisfied.

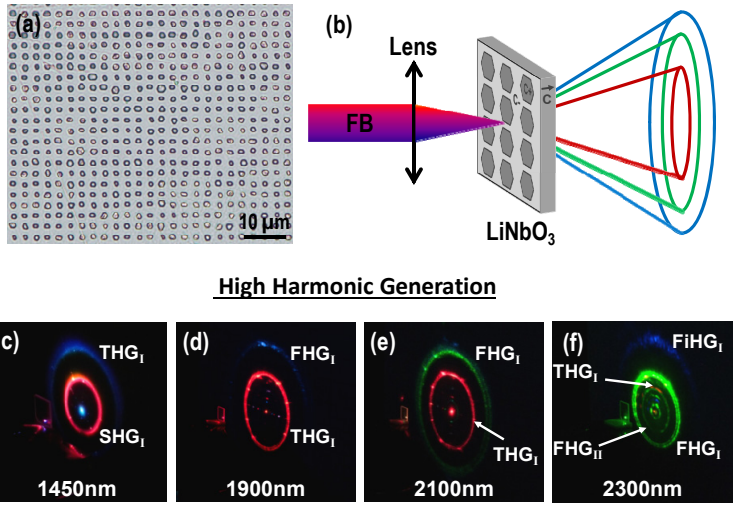

Fig. 1. (a). Optical picture of a square lattice of inverted ferroelectric domains in $LiNbO_3$. The period of the structure is Λ~2 μm. (b) Schematic of the experimental set-up for conical high harmonic generation process for an incident fundamental beam along the z axis of the crystal. (c-f) Experimental images of multiple high-harmonic conical beams recorded in the far field when the fundamental wavelength was fixed at 1450, 1900, 2100 and 2300nm, respectively.

Two different types of nonlinear processes can account for the observed non-collinear $\chi^{(2)}$-cascade high harmonic generation depending whether the sum frequency mixing (SM) occurs via transverse or longitudinal PM conditions. The nonlinear Cerenkov radiation represents the type of nonlinear interaction in which only the longitudinal PM condition is fulfilled. In this case, the conical angle is defined by the material refractive index dispersion and multiple high harmonic generation is obtained by SHG and successive sum frequency conversion processes between the longitudinal component of the generated harmonics and the fundamental beam. This process is known as Type I Cerenkov harmonic generation. Besides, the longitudinal PM condition can also be fulfilled by sum frequency mixing processes between the collinearly generated SHG and THG and the fundamental beam. This process is labelled as type II Cerenkov harmonic generation. The phase matching conditions for both types of $\chi^{(2)}$-Cerenkov cascade generation can be written as:

$$Type\ I \qquad k_{(i+1)\omega}\cos\theta^{I}_{(i+1)} = k_{i\omega}\cos\theta_i + k_{\omega} = (i+1)\cdot k_{\omega} \qquad (1)$$

$$Type\ II \qquad k_{(i+1)\omega}\cos\theta^{II}_{(i+1)} = k_{i\omega} + k_{\omega} \qquad (2)$$

where k_ω and $k_{i\omega}$ are the fundamental and the i-th order harmonic wave vector respectively, and θ_i the internal conical angle of the i-th order Cerenkov harmonic generated wave.

#179795 - $15.00 USD Received 12 Nov 2012; revised 8 Dec 2012; accepted 17 Dec 2012; published 21 Dec 2012

Superscripts I and II refer to the Cerenkov-type process. Figure 2(a) shows the schematic diagrams of Type I and Type II multistep cascaded $\chi^{(2)}$ –Cerenkov harmonic generation.

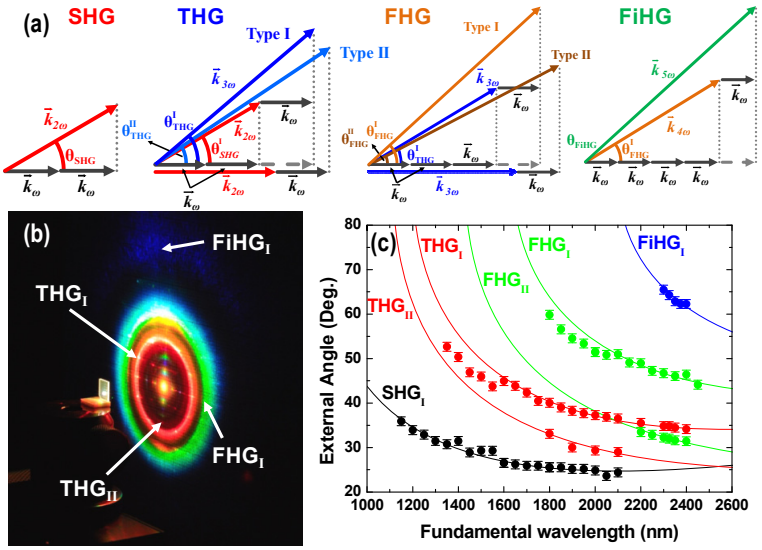

Fig. 2. (a). Schematic diagram showing the longitudinal phase matching condition of the multistep cascaded $\chi^{(2)}$ –Cerenkov harmonic generation via Type I and Type II processes for the different harmonics observed in this work. (b) Multicolor ring-shaped Cerenkov multiple high harmonic generation recorded in the far field when the fundamental beam was tuned at 2100 nm. Red, green and blue conical emissions are simultaneously obtained via multistep frequency tripling, quadrupling and quintupling of the fundamental wave. (c) Angular dependence of the generated harmonic beams as a function of the fundamental wavelength. Theoretical calculations and experimental points are represented by solid lines and dots respectively.

As a representative example Fig. 2(b) shows a colourful ring shaped nonlinear pattern recorded in the far field when the fundamental beam was tuned at 2100 nm. Red, green and blue conical beams are simultaneously obtained via multistep Type I frequency tripling, quadrupling and quintupling of the fundamental wave: the third harmonic generation results from a two step process that involves conical SHG and successive sum frequency mixing between the longitudinal component of SHG and the fundamental incident wave; similarly, the 4th and 5th harmonic conical beams are produced by sum frequency mixing the longitudinal component of the third and fourth harmonic, respectively, and the fundamental wave. Additionally, an extra red ring with a weaker intensity is also observed and has been assigned to the type II Cerenkov sum-frequency mixing between the collinear SHG and the incident beam (See Fig. 2(a)). We note that the SHG conical wave is barely observed in Fig. 2(b) due to experimental limitations of our digital camera in the 2μm infrared region. The external measured angles obtained by tuning the fundamental wavelength in the 1200-2400 nm spectral range are shown in Fig. 2(c). The generated conical emissions show a decreasing angle with increasing wavelength in agreement with the index dispersion of $LiNbO_3$. The theoretical fittings to Eqs. (3) and 4 associated with the different Cerenkov harmonic generation processes (from 2th to 5th) are plotted as solid lines according to the expressions:

$$\cos\theta^{I}_{(i+1)} = \frac{(i+1)\cdot k_{\omega}}{k_{(i+1)\omega}} = \frac{n_{\omega}}{n_{(i+1)\omega}} \tag{3}$$

$$\cos\theta^{II}_{(i+1)} = \frac{k_{i\omega} + k_{\omega}}{k_{(i+1)\omega}} = \frac{i\cdot n_{i\omega} + n_{\omega}}{(i+1)\cdot n_{(i+1)\omega}} \tag{4}$$

#179795 - $15.00 USD Received 12 Nov 2012; revised 8 Dec 2012; accepted 17 Dec 2012; published 21 Dec 2012

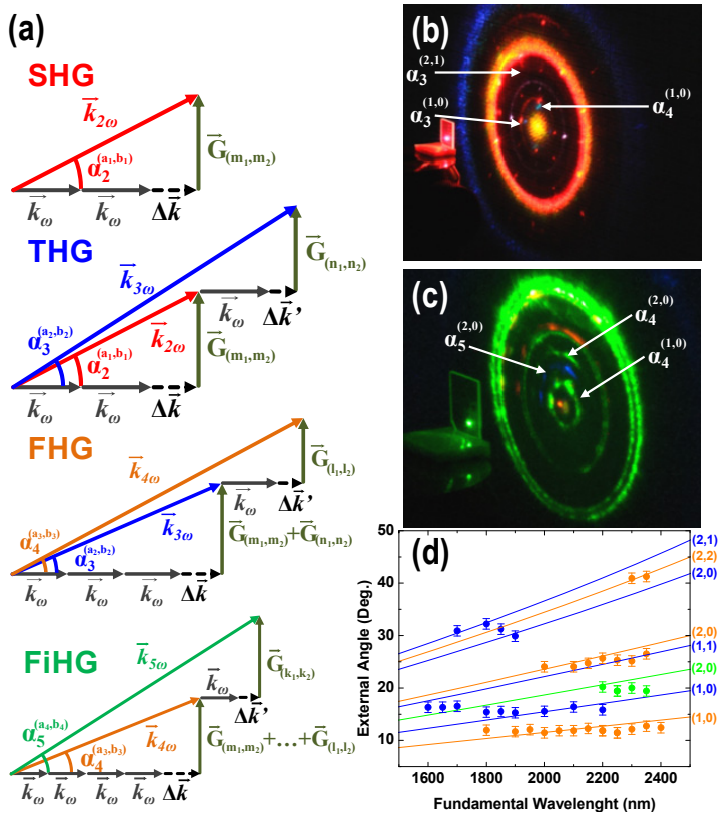

Fig. 3. (a). Schematic diagram showing the transverse phase matching condition of the multistep cascaded $\chi^{(2)}$-nonlinear Raman Nath diffraction for the different harmonic generation processes observed in this work: Second Harmonic Generation (SHG), Third Harmonic Generation (THG), Fourth Harmonic Generation (FHG) and Fifth Harmonic Generation (FiHG). (b,c) Far field nonlinear patterns recorded when the fundamental beam was fixed at 1900nm and 2300nm, respectively. The inner rings have been labelled as $\alpha_i^{(a,b)}$ where "i" correspond to the harmonic order (i = 2,...5) and (a,b) is the order of the NLRN process involved. (d) Angular dependence of the generated conical NLRN patterns as a function of the fundamental wavelength. Theoretical fittings (solid lines), experimental data (coloured dots). Blue, orange and green lines correspond to 3th, 4th and 5th harmonics, respectively.

which are directly derived from Eqs. (1) and (2). The relationship between the external and internal angle was obtained by means of Snell's equation using the ordinary refractive index values given by Zelmon *et al* [21]. A good agreement was obtained between the experimental and theoretical curves for both type I and II longitudinal PM conditions. Similar results were obtained for the extraordinary beam. Both types of Cerenkov frequency conversion processes have been already studied for conical beams, however the maximum harmonic order was limited to THG [22–24]. Here, the conical Cerenkov harmonic generation is extended up to fifth order owing to the large density of ferroelectric domain walls at the irradiated areas and the small size of the inverted domains (~1μm). In fact, the great variety of reciprocal lattice vectors provided by both, the nonlinear $\chi^{(2)}$ square modulation and the ferroelectric domain walls along with the additional random components arising from the imperfections on the size and shape of the hexagonal individual domains, make possible to compensate the mismatch of the Cerenkov type harmonic generation in a quasi-continuous set of directions in the XY plane [19, 25]. As a result, a large number of simultaneous phase matching conditions are available so that high harmonic generation becomes an efficient fully phase matched process exhibiting annular distribution at well defined directions governed by the longitudinal phase matching condition (Cerenkov angles).

#179795 - $15.00 USD Received 12 Nov 2012; revised 8 Dec 2012; accepted 17 Dec 2012; published 21 Dec 2012

Further, the generation of high harmonic conical waves via the so-called Nonlinear Raman Nath Diffraction (NLRN) in 2DNLPC is also observed from our structures. In this case, only the transverse PM condition is fulfilled, the angular dispersion being governed by the exact matching of the lattice period with the generated harmonic wave [26]. The second order nonlinearity induced by domain walls plays a key role in NLRN diffraction processes, however, short lattice period are required for simultaneously phase matching multiple nonlinear interactions. Similar to the Cerenkov type, NLRN high harmonic generation occurs via multistep $\chi^{(2)}$ cascade processes. In the first step, a second harmonic wave is generated satisfying the transverse PM condition: $k_{2\omega}\sin\alpha_2^{(m_1,m_2)} = \left|G_{m_1,m_2}\right| = \sqrt{m_1^2+m_2^2}G_0$ where $k_{2\omega}$ is the wave vector of the second harmonic beam, $G_0 = 2\pi/\Lambda$ being Λ the period of the nonlinear structure, $m_{1,2}$ integer numbers representing the order of the reciprocal lattice vector, and $\alpha_2^{(m_1,m_2)}$ the internal propagation angle of the (m_1,m_2)-order second harmonic wave. The next steps for the cascade generation involve the consecutive sum frequency mixing processes between the generated harmonics and the fundamental wave. The PM conditions for these successive steps can be written by the scalar relations:

$$k_{3\omega}\sin\alpha_3^{(a,b)} = \left|\vec{G}_{m_1,m_2}+\vec{G}_{n_1,n_2}\right| = \sqrt{(m_1+n_1)^2+(m_2+n_2)^2}G_o \qquad (5)$$

$$k_{i\omega}\sin\alpha_i^{(a_i,b_i)} = \left|\vec{G}_{m_1,m_2}+\vec{G}_{n_1,n_2}+...\right| = \sqrt{(m_1+n_1+...)^2+(m_2+n_2+...)^2}G_o \qquad (6)$$

$k_{i\omega}$ being the wave vector of the i-th harmonic order and $\alpha_i^{(a.b.)}$ the internal propagation angle of the i-th harmonic beam generated at order (a,b). The particular schematic PM diagram for each harmonic process is depicted in Fig. 3(a). Figure 3(b) and 3(c) show an expanded view of the far field nonlinear patterns recorded when the fundamental beam was fixed at 1900nm and 2300nm, respectively. In addition to the longitudinal PM Cerenkov harmonic beams, a set of inner rings can be observed and related to third, fourth and fifth harmonic waves. They have been labelled as $\alpha_i^{(a,b)}$ where "i" refers to the harmonic order (i = 2,...5) and (a,b) represents the reciprocal lattice vector responsible for the diffraction involved. The external angles measured on tuning the fundamental wavelength from 1600 to 2400 nm are shown in Fig. 3(d). The

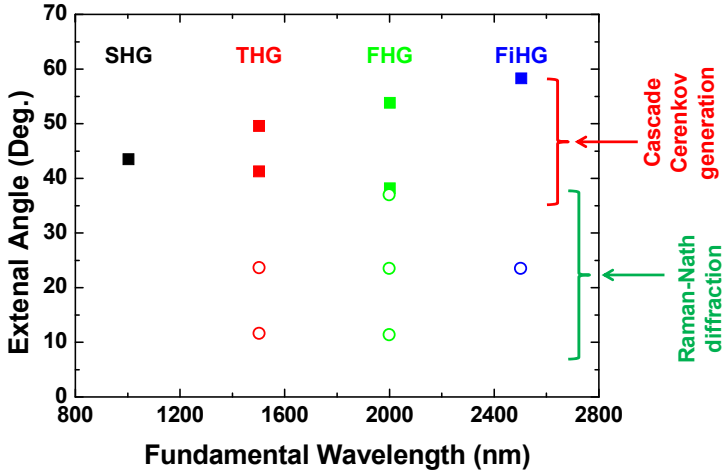

Fig. 4. Experimentally obtained external conical angles for a frequency converted wavelength of 500 nm by different types of phase matching geometries. Solid dots: Cerenkov type high harmonic generation. Open circles: Nonlinear Raman Nath diffraction processes.

#179795 - $15.00 USD Received 12 Nov 2012; revised 8 Dec 2012; accepted 17 Dec 2012; published 21 Dec 2012

theoretical angles obtained from Eqs. (5) and (6) fit well the experimental data. Here, it is worth to highlight the co-existence of both, NLRN and Cerenkov nonlinear phenomena, which allows to generate multiple harmonic conical waves at different angles.

In particular, for a frequency converted wavelength in the green-blue spectral region, angular dispersion values from 40° to 50° degrees are obtained. Similarly, several wavelengths can be generated at a fixed conical angle. Figure 4 shows a collection of all the measured external conical angles at 500 nm. Finally, the effect of the polarization of the fundamental beam on the generated nonlinear patterns was analyzed in Fig. 5. Figure 5(a-d) shows four pictures of Cerenkov type third and fourth conical rings recorded for several angles of input linear polarization. Figure 5(e-f) shows the polarization dependence of fifth and fourth Cerenkov rings along with a set of inner rings arising from NLRN diffraction processes. The results are in excellent agreement with the azimuthal dependence of the quadratic nonlinear effective coefficients of $LiNbO_3$ [19, 20, 22]. As seen, the azimuthal position of the maxima and minima of each harmonic conical wave depends equally on the orientation of input polarization regardless the involved PM condition. Moreover, complementary nonlinear patterns are obtained for linearly polarized fundamental beams with polarization states parallel to *x* and *y* axis of the crystal. So, the interaction of a circularly polarized fundamental beam would results into symmetrical conical nonlinear diffraction patterns with a homogenous intensity distribution across the whole ring [20].

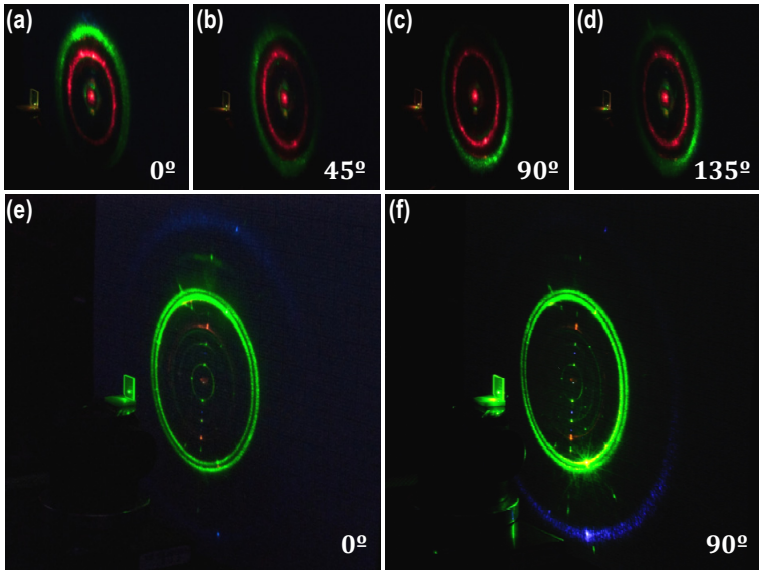

Fig. 5. Effect of the polarization of the fundamental beam on the generated nonlinear patterns.(a-d) Third and fourth Cerenkov harmonic waves for different linear polarization angles. From left to right: γ = 0°, 45°, 90° and 135°, respectively. (e-f) Far field nonlinear patterns obtained for linearly polarized fundamental beams with polarization states parallel to *x* (γ = 0°) and *y* axis (γ = 90°) of the crystal. Fourth and fifth Cerenkov rings along with a set of inner rings arising from NLRN diffraction processes can be distinguished.

4. Summary and conclusions

To summarize, careful processing based on e-beam lithography and poling of $LiNbO_3$ has allowed lateral periodic arrangements to be fabricated at pitches beyond the state of the art. This has demonstrated a step forward in the range of harmonic generation with currently available broadband sources in the VIS-NIR. Broadly tunable multiple high-harmonic conical beams have been generated by means of a multistep $\chi^{(2)}$ cascade processes in a single 2DNLPC with a square lattice of inverted domains with periodicity around 2 μm. The large density of ferroelectric domain walls at the irradiated areas combined with the small size and

#179795 - $15.00 USD Received 12 Nov 2012; revised 8 Dec 2012; accepted 17 Dec 2012; published 21 Dec 2012

dispersion of the inverted individual domains have made possible the access to a large number of QPM conditions. As a result, the simultaneous generation of multiple annular harmonics (from second up to fifth harmonic conical beams) in a single nonlinear structure is demonstrated to be an efficient phase matched process. The frequency response can be tuned in an extremely large spectral range and continuous generation of nonlinear conical beams covering the whole visible spectral region is demonstrated. Further, the same wavelength can be generated at multiple orders hence leading to concentrically emitted conical beams exhibiting angular dispersion values as large as $\Delta\theta = 50°$. To the best of our knowledge this is the first report in which on a solid state system up to fifth harmonic generated conical beams are obtained by simultaneously phase match both longitudinal and transverse geometries. The generation of conical beams has recently shown a broad number of potential applications in a wide variety of fields including optical deflection, symmetry studies, high resolution optical microscopy, or even photon entanglement [27–30]. Thus, the ability to control the spatial and spectral distribution of several photons simultaneously on a compact system represents a step towards novel nonlinear color fan devices, and will enable new experiments on, for example, quantum optics or 3D in-vivo imaging.

Acknowledgments

This work was supported by EU FP7 NoE Nanophotonics4Energy Grant No. 248855, the Spanish MICINN CSD2007-0046 (Nanolight.es), MAT2009-07841 (GLUSFA), MAT2010-17443 and Comunidad de Madrid (Grant S2009/MAT-1756 PHAMA).

#179795 - $15.00 USD Received 12 Nov 2012; revised 8 Dec 2012; accepted 17 Dec 2012; published 21 Dec 2012